Identification of the different orders of scattering in α-nucleus reactions

J. Duflo
Institut National de Physique Nucléaire et de Physique des Particules, Laboratoire National Saturne, Saclay, France
(Received 2 September 1986)

Up to the highest momentum transfer measured [$\simeq 2$ (GeV/c)^2], the inelastic double differential α-nucleus cross sections obtained with α's of 7 GeV/c incident momentum are fairly well described by an incoherent sum of single and double quasielastic collisions on the substructures of the target, and the different orders of scattering are clearly identified. The assumptions used in this analysis are also justified by the elastic behavior of the integrated partial cross sections that correspond to these different orders of scattering. The interpretation of these integrated cross sections by a Glauber model enables the evaluation of the mean square radii as well as the spectroscopic factors of the substructures concerned. Pion processes measured in these α-nucleus collisions are also considered.

INTRODUCTION

We proposed a first description of the inclusive inelastic cross sections in terms of an incoherent sum of quasielastic scattering processes of α projectiles on the substructures of the ^{4}He target for the reaction $\alpha\alpha \rightarrow \alpha X$, measured with α's of 4.3 and 5.07 GeV/c incident momentum.[1] The main trends of these data were also well reproduced by multiple scattering models,[2-5] but these calculations could not explain a part of their behavior, which some authors[5] attributed to more complex reaction mechanisms or to clusters in the nuclei.

New measurements at 7 GeV/c with ^{2}H, ^{3}He, and ^{4}He targets[6] enable us to confirm and extend our analysis up to the highest momentum transfer measured [$|t| \simeq 2$ (GeV/c)^2]. In this case, the different orders of scattering are clearly identified in the energy loss spectra. As a result of the precision of these new data and the wider range of transfer momenta measured, double scattering contributions are displayed. A method similar to that used to describe the simple quasielastic scattering is also used to study this process. On the other hand, the energy loss spectra measured include part of the one pion production field. Measurement of this inelastic reaction with a ^{1}H target is presented,[7] but here it is shown that this pion contribution can also be described by a pattern similar to the one proposed for the double scattering contributions. In this way, pion production with ^{2}H, ^{3}He, and ^{4}He targets is evaluated by comparing the corresponding inelastic spectra with the αp inelastic data.

First, we present the method used to describe all the inclusive double differential cross sections. Next, we show the integrated partial cross sections that correspond to the different orders of scattering. The technique used in the analysis is based mainly on *elastic* kinematic calculations and it is justified by its successful description of all the data, but also by the characteristic *elastic* behavior of the partially integrated spectra. As will be seen, some understanding of the behavior of the partial cross sections can be obtained without theory both by the comparison of the results of different targets (^{1}H, ^{2}H, ^{3}He, and ^{4}He) and by the comparison of these inelastic cross sections with their elastic counterparts (already published[8]).

At low momentum transfer, the interpretation of the quasielastic integrated cross sections by a Glauber model,[9] which successfully accounts for elastic scattering between light nuclei in the same range of momentum transfer, as was shown in our previous publications on nuclei reactions,[1,8,10] allows us to calculate the spectroscopic factors of the components of the targets and the mean square radii of the polybaryonic substructures scattered.

I. DESCRIPTION OF THE DOUBLE DIFFERENTIAL INELASTIC SPECTRA

The inelastic spectra measured at 7 GeV/c are described by two contributions:

(i) a quasielastic part which is always the more important part of the spectrum measured in the momentum range of the scattered α, and

(ii) a pion production part which is 20–30 times weaker than the quasielastic part. Pion production associated with a nucleon (the other part of the target being assumed as spectator) takes place at t values outside the quasielastic spectrum and therefore can be studied.

A. Quasielastic part of the spectra

As can be seen in Figs. 1–3, most of the data are well fitted by an incoherent sum of quasielastic scatterings on the target and on the substructures of the target. Only two modes of quasielastic reaction are taken into account:

(i) simple elastic scattering on a substructure, the other being spectator (spectra labeled 1–3), and

(ii) quasielastic scattering on the target or on a substructure of the target, both being broken up into two parts in the final state (spectra labeled 4–6).

1. Calculation of the partial spectra

The forms of the partial spectra, that is, the distributions of the α's as a function of the energy loss ΔE due to the breakup of the target and to the Fermi momenta acquired by the components of the target during the reaction, are obtained by a simulation (Monte Carlo method). The variables used in this simulation are the directions and sizes of the Fermi momenta.

For *simple* α scattering on a substructure with a spectator, each simulated event corresponds to an elastic scattering between a substructure with momentum $\mathbf{p}_f$ (c.m. of the target) and an α particle with a momentum calculated kinematically so that conservation of energy and momentum is globally respected in the reaction. The energy carried away by the spectator is $E_{sp}=(m_{sp}^2+p_f^2)^{1/2}$, and the only energy available for the "elastic" scattering of the α is $E'=E_T-E_{sp}$, where E_T is the total energy of the system.

For *double* α scattering on a target or on a substructure of the target, the kinematics of a simulated event correspond to those of an α elastic scattering on a "missing mass," whose value is equal to the sum of the energies of the two components of the scattered element; that is,

$$MM=(M_1^2+p_f^2)^{1/2}+(M_2^2+p_f^2)^{1/2},$$

where M_1 and M_2 are the masses of these components, and $\mathbf{p}_f$ their Fermi momenta acquired in the breaking up of the scattered element. MM does not depend on the energy transferred for the elastic scattering (Fermi momenta of the two components are equal and opposite in direction). Once again, the momentum of the α scattered "elastically" and the energy available in the elastic part of the reaction are calculated such that energy and momentum are conserved globally.

When double scattering occurs on a substructure, therefore with a spectator, the values $\mathbf{p}'_f$ of the spectator (and of the substructure) and $\mathbf{p}_f$ of the components of the substructure do not depend on each other and may have different distributions. This is obviously taken into account in the simulation.

The double differential cross sections $d^2\sigma/d\omega\,dp$ are evaluated by fitting the heights of the partial spectra to the data, the adjustment being checked by a χ^2 method.

Distributions of Fermi momenta: The angular distribution of the Fermi momenta is assumed to be isotropic in the center of mass of the target. For $\alpha\alpha$ reactions, the p_f distributions of the substructures taking part in the reaction, (t,N) or (d,d), are the same as those used to de-

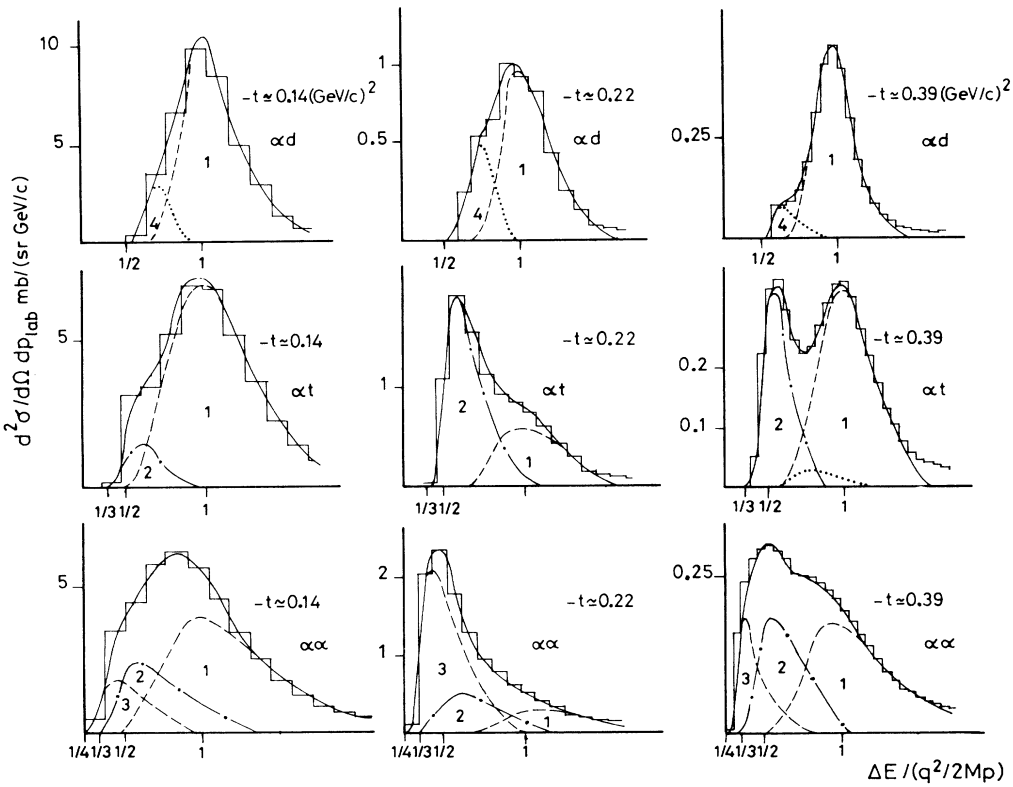

FIG. 1. Inclusive cross sections $d^2\sigma/d\Omega\,dp$ (lab) for the reactions $\alpha\,{}^2\mathrm{H}\rightarrow\alpha\mathrm{X}$, $\alpha\,{}^3\mathrm{He}\rightarrow\alpha\mathrm{X}$, and $\alpha\,{}^4\mathrm{He}\rightarrow\alpha\mathrm{X}$ at 7 GeV/c. Elastic peaks are subtracted. For each column, the spectra are measured at the same angle for each target [$\theta_{lab}=3.1°$, 3.8°, and 5.1° corresponding to transfer momenta $|\bar{t}|=0.14$, 0.22, and 0.39 (GeV/c)^2]. These spectra are analyzed as an incoherent sum of quasielastic scatterings. The partial spectrum 1 corresponds to $\alpha\mathrm{A}\rightarrow\alpha\mathrm{N}$ + spectator, A being ^{2}H, ^{3}He, or ^{4}He and N a nucleon of the target; 2 corresponds to $\alpha\mathrm{A}\rightarrow\alpha\mathrm{d}$ + spectator; 3 corresponds to $\alpha\mathrm{A}\rightarrow\alpha\mathrm{t}$ + spectator, t being ^{3}He or ^{3}H; 4 corresponds to $\alpha\mathrm{A}\rightarrow\alpha(2\mathrm{N})$ (+ spectator if A is ^{3}He or ^{4}He: it is a scattering on a dibaryon of the target, broken up into two nucleons). The solid line represents the sum of these contributions.

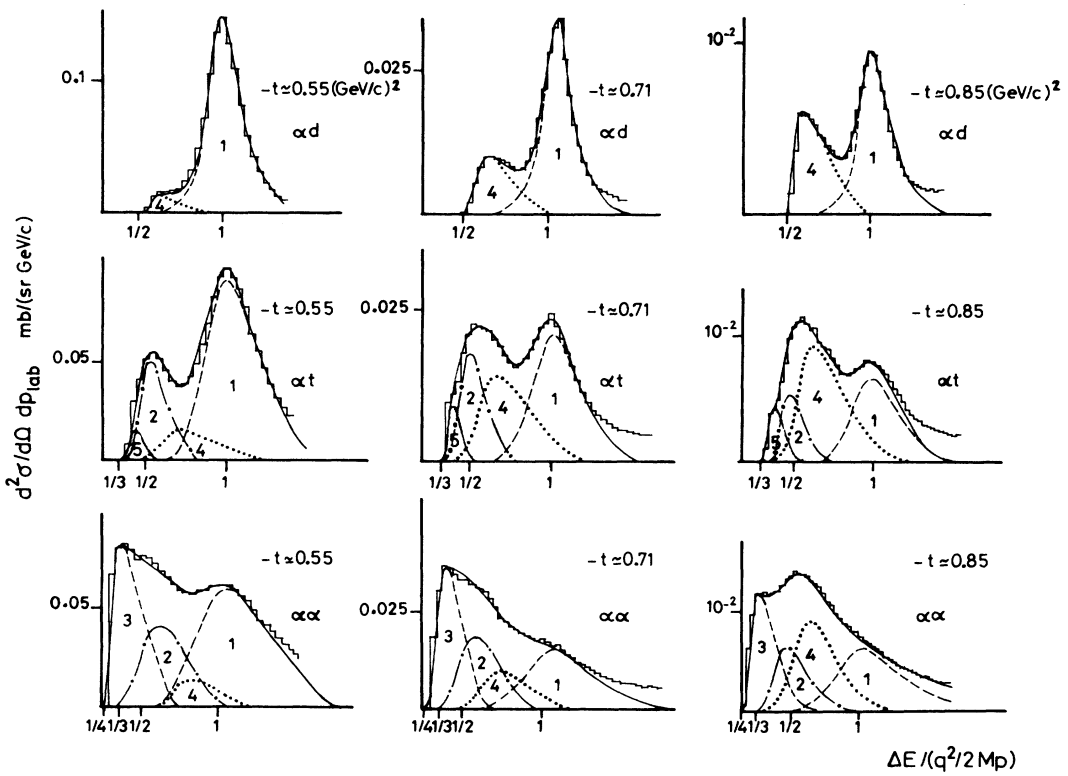

FIG. 2. Same as for Fig. 1, but $\theta_{lab}=6.1°$, 6.9°, and 7.6°, corresponding to transfer momenta $|\bar{t}|=0.55$, 0.71, and 0.85 $(GeV/c)^2$. The spectra labeled 5 correspond to double scattering on a tribaryon of the target, broken up into a deuteron and a nucleon. With a ^4He target, the tribaryon is a substructure of the target and a nucleon is the spectator.

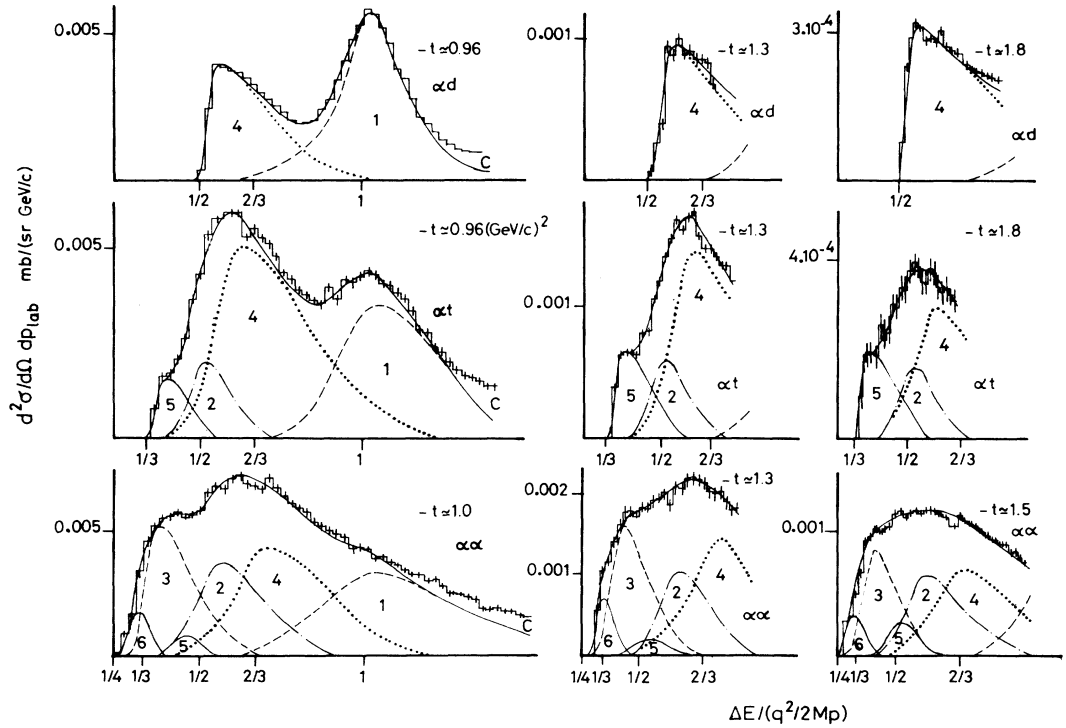

FIG. 3. Same as for Figs. 1 and 2, at higher transfer momenta [$\theta_{lab}=8.2°\rightarrow |\bar{t}|=0.96$ $(GeV/c)^2$; $\theta=9.5°\rightarrow |\bar{t}|=1.3$ $(GeV/c)^2$; $\theta=10.1°\rightarrow |\bar{t}|=1.5$ $(GeV/c)^2$; and $\theta=11.1°\rightarrow |\bar{t}|=1.8$ $(GeV/c)^2$]. The spectra labeled 6 correspond to $\alpha\,^4He\rightarrow\alpha$(d,d) or α(t,N), double scattering on two substructures of ^4He.

scribe the $\alpha\alpha$ data at 4.3 and 5.07 GeV/c.[1]

For α ^{3}He reactions, the p_f distribution for the substructures d and p in ^{3}He is the Irving-Gunn distribution,[11] and the classical Hülthen function is used for the nucleons in a deuteron target. In fact, fitting the calculated partial spectra to the data at 7 GeV/c does not require very sophisticated momentum distributions.

Gaussian functions in momentum space $\phi(p) = A \exp(-p^2/2p_0)$, with a suitable parameter p_0, enable us to obtain results differing insignificantly from those obtained with more sophisticated distributions. The appropriate values of p_0 for substructures in ^{2}H, ^{3}He, and ^{4}He are 45, 90, and 135 MeV, respectively, which is approximately equal to the mean square momentum $\langle p^2 \rangle^{1/2}$ corresponding to the distributions chosen.

Finally, a Gaussian spread is introduced into the calculations to take into account the resolution of the spectrometer ($\Delta p/p \simeq 0.2\%$) and the angular aperture (2×10^{-4} sr).

2. *Results*

A selection of α-nucleus spectra measured at 7 GeV/c incident momentum are presented in Figs. 1–3, along with calculated partial quasielastic spectra. In each column the angles measured with ^{4}He, ^{3}He, and ^{2}H targets are equal or very close (measurements were made in the same experimental conditions).

Partial spectra labeled 1, 2, and 3 correspond to scattering on substructures containing one, two, and three nucleons respectively, and with a spectator. Spectra labeled 4–6 correspond to the α's being quasielastically scattered on two substructures of the target. Spectrum 4 represents α scattering on a dibaryon broken up in the final state, and with a spectator when the target is ^{3}He or ^{4}He, 5 corresponds to α scattering on a tribaryon broken up into a nucleon and a dibaryon (and with a spectator if the target is ^{4}He), and, finally, 6 corresponds to α scattering on ^{4}He broken up into two substructures d + d or t + N. The sums of partial spectra are represented by solid lines. The spectra presented in Figs. 1–3 are plotted as a function of a dimensionless ratio $\rho = \Delta E/(q^2/2M_p)$, where ΔE is the energy loss, $q^2 \simeq -t$ the momentum transfer corresponding to the scattering angle measured, and M_p the proton mass. The use of this unit makes comparison of the spectra easier; this is true both for the various targets and the scattering angles, since the elastic peaks for an A target (A denotes atomic number) are always centered on the position $\rho = 1/A$, which also applies to quasielastic bumps.

No interference contribution has been taken into account in the fits of the spectra and, *a posteriori*, the result justifies this incoherent summation of these partial spectra.

In Table I all partial contributions used to describe quasielastic spectra have been presented, both for the various targets and as a function of the momentum transfer t.

Remark: The double scattering spectra 4–6 may contribute to the inelastic spectra at transfer momenta lower than those indicated in Table I, but these contributions are then very weak compared to the simple scattering contributions and cannot be evaluated correctly by the method used here.

B. Pion contributions

αp inelastic spectrum: Results for this reaction at 7 GeV/c are presented elsewhere,[7] but no explanation has been given for the *form* of the double differential spectra measured. One of these spectra is presented in Fig. 4(a). The similarity between these spectra and the double scattering already presented (4 in Figs. 1–3) suggests similar quasielastic behavior of this inelastic reaction. Indeed, in the same way as the α(2N) spectrum—double scattering of an α particle on the two nucleons of the deuteron—can be described as an elastic scattering of an object of missing mass

$$M_{(2N)} = (m_p^2 + p_f^2)^{1/2} + (m_n^2 + p_f^2)^{1/2} ,$$

m_p and m_n being the masses of a proton and a neutron and p_f their Fermi momentum, we propose to describe the pionic spectrum by an α quasielastic scattering on a (pπ) system of missing mass

$$M_{(p\pi)} = (m_p^2 + p_f'^2)^{1/2} + (m_\pi^2 + p_f'^2)^{1/2} ,$$

each of the components of this system being a Fermi momentum p_f'. As can be seen in Fig. 4(a), a good fit for

TABLE I. Composition of the quasielastic spectra. (Underlined numbers correspond to labels of the partial quasielastic spectra seen in Figs. 1–3.) (sp. denotes spectator.)

	$-t \geq 0.06$	$-t \geq 0.15$	$-t \geq 0.4$	$-t \geq 0.5$	$-t \geq 0.9$ (GeV/c)^2
αd→	αN + N sp. (1)	α(2N) (4)			
α ^{3}He→	αp + d sp. (1) αd + p sp. (2)		α(2N) + N sp. (4)	α(d,p) (5)	
$\alpha\alpha$→	αN + t sp. (1) αd + d sp. (2)			α(2N) + d sp. (4)	α(d,N) + N sp. (5) α(t,N) α(d,d) (6)
	αt + N sp. (3)				

this data is thus obtained, the p_f' distribution corresponding to a simple Gaussian function $\psi(p_f')=\psi_0\exp(-p_f'^2/2p_\pi^2)$, $p_\pi=135$ MeV/c.

We make the following remarks:

(1) In the kinematic calculations of these inelastic spectra, the energy required to produce a pion is accounted for.

(2) As will be seen, the quasielastic description of this reaction is confirmed by the quasielastic behavior of the corresponding integrated spectrum (Fig. 10).

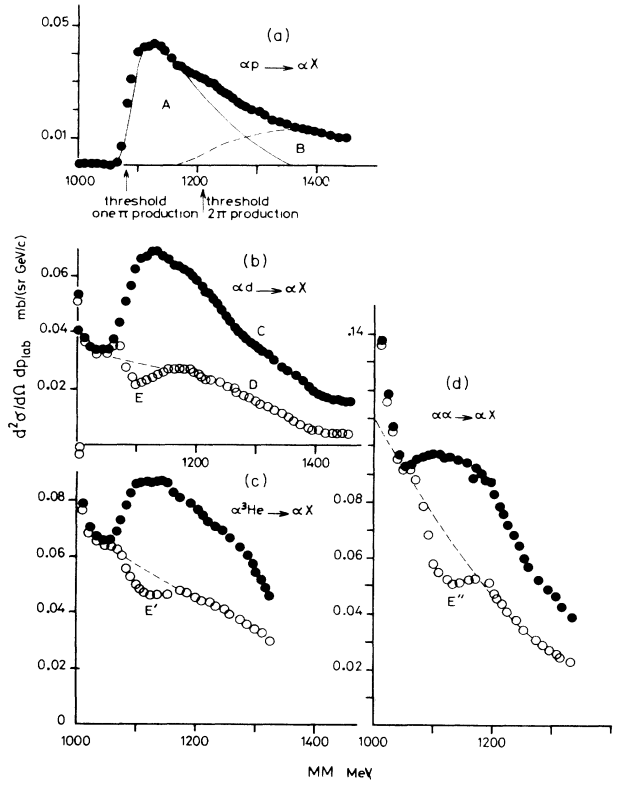

FIG. 4. Double differential inelastic cross sections at $\theta_{lab}=4°$ beyond the pion production threshold for (a) $\alpha p\rightarrow\alpha X$, (b) $\alpha\,^2H\rightarrow\alpha X$, (c) $\alpha\,^3He\rightarrow\alpha X$, and (d) $\alpha\,^4He\rightarrow\alpha X$. The scale of missing masses is calculated for αN reactions, N being a proton or nucleon of the target, the mass of the spectator next to N not being taken into account. In (a) the spectrum A represented by a solid line is the result of a kinematic calculation described in the text. The spectrum B [in (a)] denoted by a dotted line is the result of subtracting the spectrum A from the data. In (b)–(d) the ○ are the results of subtracting the inelastic spectrum $\alpha p\rightarrow\alpha X$ from the spectra obtained with the other targets. This background may be attributed to pion contribution associated with multibaryonic substructures or with the target. The "structures" E, E', and E'' probably have no real signification. They are due to the subtraction of the $\alpha(p,\pi)$ spectrum obtained with a ^1H target and would certainly disappear if an $\alpha(N,\pi)$ spectrum widened by the Fermi momentum of the nucleon N of the multibaryonic target were more correctly subtracted.

(3) When $p_f=p_\pi$, the corresponding missing mass $M=1140$ MeV/c is the same as that proposed in Ref. 7 for the (N,π) system.

(4) One result that appears when the calculated spectrum is subtracted from the data spectrum [Fig. 4(a)] is an inelastic contribution beginning at the threshold of $(p,2\pi)$ production.

Pion production with other targets: As can also be seen in Fig. 4, in the same range of energy loss, the inelastic spectra of $\alpha\,^2H$, $\alpha\,^3He$, and $\alpha\,^4He$ scattering behave as the αp spectrum.

The analysis of these data is more difficult for two reasons:

(i) the widening of the αN quasielastic peak when the target is heavier (N being a nucleon substructure in the target), and

(ii) the probability of the existence of additional pion production associated with the substructures composed of several nucleons, or with the target itself.

In Fig. 4 the cross sections are plotted as a function of the missing masses, the inelastic processes are considered as being associated with a nucleon N of the target, and the mass of the spectator is disregarded. The four inelastic spectra appear in the same "missing mass' range.

Assuming that the cross sections for the inelastic contribution $\alpha A\rightarrow\alpha(N\pi)$ + spectator $(A\rightarrow\,^2H,\,^3He,$ or $^4He)$ are equal to those of the inelastic reaction $\alpha p\rightarrow\alpha(p,\pi)$, the inelastic spectrum $\alpha p\rightarrow\alpha X$ has been subtracted from the other $\alpha\,^2H$, $\alpha\,^3He$, and $\alpha\,^4He$ spectra for missing masses higher than the threshold for one pion production. The spectrum resulting from this subtraction can be understood as the end of another pion production spectrum associated with a heavier "target" (the threshold of one pion production associated with a target of several nucleons is higher than that associated with one nucleon). This weak inelastic contribution cannot be separated from the important nonpion quasielastic bump.

Remark: The hypothesis of an identical π production associated with a nucleon for all light targets must be linked to the fact that the "spectroscopic factor" of the N substructure in these targets is equal to 1, as can be seen in Fig. 5.

II. PARTIALLY INTEGRATED CROSS SECTIONS $d\sigma/dt$

In Figs. 5–10 the integrated partial spectra corresponding to the different contributions of the inelastic spectra measured are presented. In these figures each point corresponds to the area of one partial spectra (1–6 in Figs. 1–3 and A in Fig. 4) as a function of the transfer t. The soundness of our first analysis of the reaction $\alpha\alpha\rightarrow\alpha X$ measured at lower energy[1] was already supported by the elastic behavior of such integrated partial spectra. This behavior is fairly well confirmed by the data at 7 GeV/c; that is, for all partial spectra resulting from this analysis.

In Fig. 5 the cross sections $d\delta/dt$, for the reactions $\alpha A\rightarrow\alpha N$ + spectator, where A is ^2H, ^3He, and ^4He, and N a nucleon of the target A, are presented with the αp

elastic cross sections measured in the same experiment. In view of the large range of cross sections presented, the superposition of the four spectra is very noticeable, even if some small differences can be observed between these results, especially at high transfers. These differences are probably due to inelastic contributions such as pion production associated with the target, or with a multibaryonic substructure. A similar effect has already been proposed to explain part of the inelastic contributions on the outside of the quasielastic bump [Figs. 4(b)–4(d)].

In Fig. 6 the reactions $\alpha A \rightarrow \alpha d$ + spectator, where A is ^{3}He or ^{4}He, are presented along with αd elastic cross sections. In Fig. 7, $\alpha\,^4\text{He} \rightarrow \alpha t + N$ spectator is presented along with the $\alpha\,^3$He elastic cross sections. All the elastic reactions were measured in the same experiment.

As can be seen, all these quasielastic integrated spectra present clearly diffractive structures in the same range of momentum transfer as the diffractive structures of the corresponding elastic spectra. The integrated double scattering cross sections corresponding to the partial spectra labeled 4–6 in Figs. 1–3 are displayed in Figs. 8 and 9.

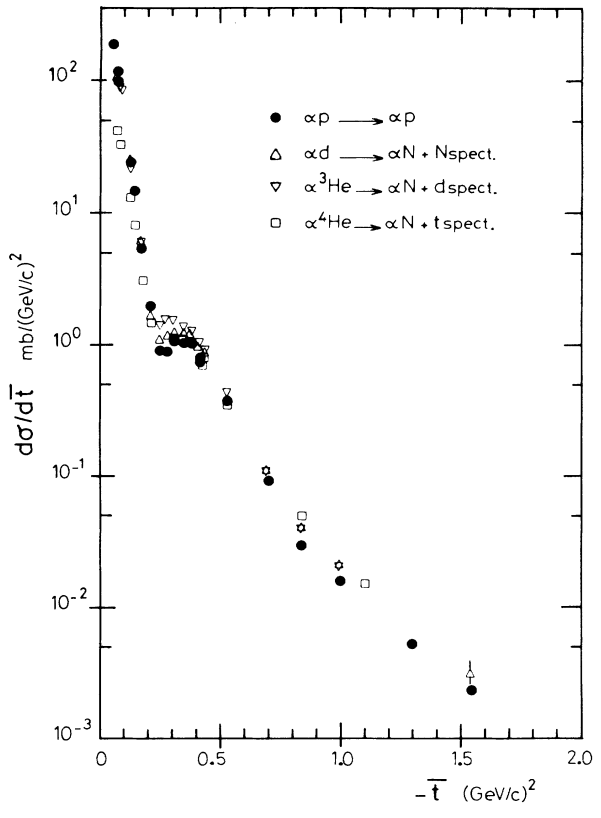

FIG. 5. $d\sigma/d\bar{t}$ integrated partial cross sections for the quasielastic reactions $\alpha d \rightarrow \alpha N + N$ spectator (△), $\alpha\,^3\text{He} \rightarrow \alpha N + d$ spectator (▽), and $\alpha\,^4\text{He} \rightarrow \alpha N + t$ spectator (□), along with the αp elastic cross sections (●), all at incident momentum 7 GeV/c.

In Fig. 8 the reaction $\alpha d \rightarrow \alpha(2N)$ is presented along with the αd elastic reaction at 7 GeV/c. Data for the same reactions obtained at 4 GeV/c (Ref. 12) are superposed and show weak incident energy dependence in this range. The similarity between the elastic and quasielastic processes seems significant.

The double scattering reaction $\alpha\,^3\text{He} \rightarrow \alpha(\text{d,p})$ is also presented in Fig. 8 along with the $\alpha\,^3$He elastic reaction obtained in the same momentum range as the triple scattering in the elastic spectrum; in the same way, $\alpha(2N)$ double scattering appears in the same range of transfer as one of the double scattering reactions in the αd elastic spectrum.

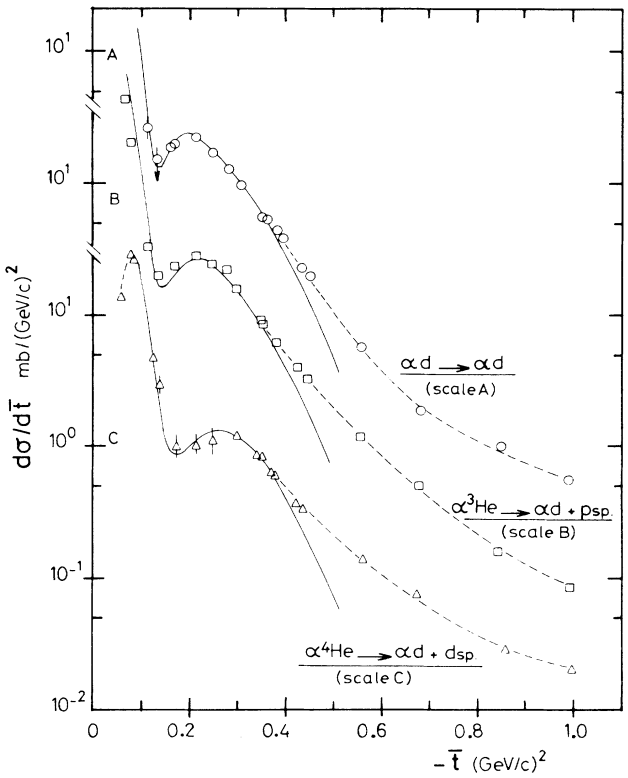

FIG. 6. $d\sigma/d\bar{t}$ integrated cross sections at 7 GeV/c for $\alpha\,^3\text{He} \rightarrow \alpha d + p$ spectator and for $\alpha\,^4\text{He} \rightarrow \alpha d + d$ spectator, along with the αd elastic cross sections. Data are separated by a factor of 10 to enhance legibility. The dashed lines are to guide the eye. The solid lines correspond to calculations based on the Czyz and Maximon model (Ref. 13), with the usual NN parameters [already used to describe elastic data at 7 GeV/c (Ref. 8)], i.e., the scattering amplitude, the Re/Im ratio $\alpha = -0.35$, the elastic scattering slope $\beta = 6$ (GeV/c)$^{-2}$, and the total cross section $\sigma = 45$ mb. The other parameters used in the calculations are R ($R^2 = \frac{2}{3}\langle r^2 \rangle$, $\langle r^2 \rangle$ being the mean square radius of the scattered object—substructure or target) and f, the spectroscopic factor or normalization factor vs elastic reaction: For $\alpha\,^3\text{He} \rightarrow \alpha d + N$ spectator, $R_2 = 1.2$ fm and $f_2 = 1$; for $\alpha\,^4\text{He} \rightarrow \alpha d + d$ spectator, $R_2 = 0.8$ fm and $f_2 = 0.5$; for αd elastic scattering, $R_d = 1.45$ fm (Ref. 15).

In Fig. 9 the reactions $\alpha A \rightarrow \alpha(2N)$ + spectator, where A is ^{3}He or ^{4}He, are presented along with $\alpha d \rightarrow \alpha(2N)$. The similarity of behavior among these three integrated spectra certainly justifies the use of an identical interpretation for the three targets ^{2}H, ^{3}He, and ^{4}He. At high momentum transfer, these contributions become very important. The $\alpha(2N)$ + spectator cross sections obtained with ^{3}He and ^{4}He targets are approximately equal to and twice those of the $\alpha(2N)$ cross sections obtained with a ^{2}H target. Once again, the diffractive structures of these new integrated spectra lend weight to the proposed analysis.

In Fig. 10 three integrated spectra $d\sigma/d\bar{t}$ are displayed:

(i) αd elastic cross sections,

(ii) $\alpha\alpha \rightarrow \alpha(2N)$ quasielastic cross sections measured in the same experiment, and

(iii) $\alpha p \rightarrow \alpha(N,\pi)$ cross sections corresponding to the calculated spectra, such as A in Fig. 4(a), which fit the αp inelastic data.

This comparison justifies understanding the inelastic process $\alpha p \rightarrow \alpha(N,\pi)$ as a double quasielastic scattering of α projectiles on to a "two component" object, in which case it is seen that replacing one of the nucleons in the dibaryon by a pion changes only the magnitude of the cross sections, the slopes and positions of the diffractive structures as a function of the momentum transfer remaining unchanged.

III. INTEGRATED INELASTIC SPECTRA

The inclusive inelastic cross sections $d\sigma/d\bar{t}$ are obtained by integrating the inelastic spectra measured over the momenta of the scattered α's. In Fig. 11 data for the α reactions with ^{2}H, ^{3}He, and ^{4}He at 7 GeV/c and with ^{4}He at 4.32 and 5.07 GeV/c are displayed. Each of these spectra presents a diffractive structure around $|\bar{t}| \simeq 0.2$ (GeV/c)^2. On the other hand, the superposition of the $\alpha\alpha$ cross sections shows that the result is independent of the incident energy in the range measured.

As can also be seen in Fig. 11, calculations in the framework of the Glauber theory[2-4] reproduce the main features of the $\alpha\alpha$ data, but some deviations are intrigu-

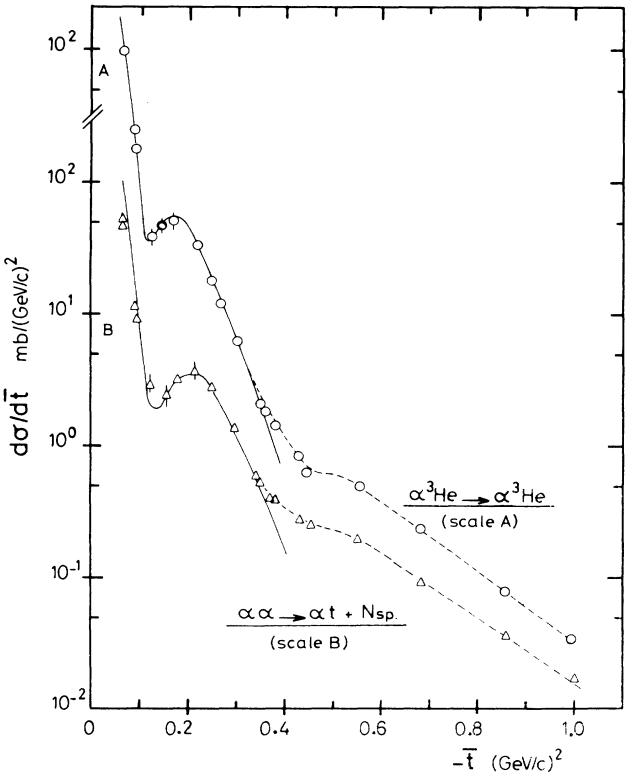

FIG. 7. $d\sigma/d\bar{t}$ integrated cross section at 7 GeV/c for $\alpha\,^4$He$\rightarrow\alpha$t + N spectator, along with $\alpha\,^3$He elastic cross sections. The dashed lines are to guide the eye and the data are spaced out to enhance legibility. The solid lines represent calculations based on the Czyz and Maximon model, with the same NN parameters as in Fig. 6. The other parameters used to describe the quasielastic cross sections at low transfers are as follows: $R_3 = 1$ fm and $f_3 = 0.5$. For elastic cross sections, $R_3 = 1.4$ fm (Ref. 1).

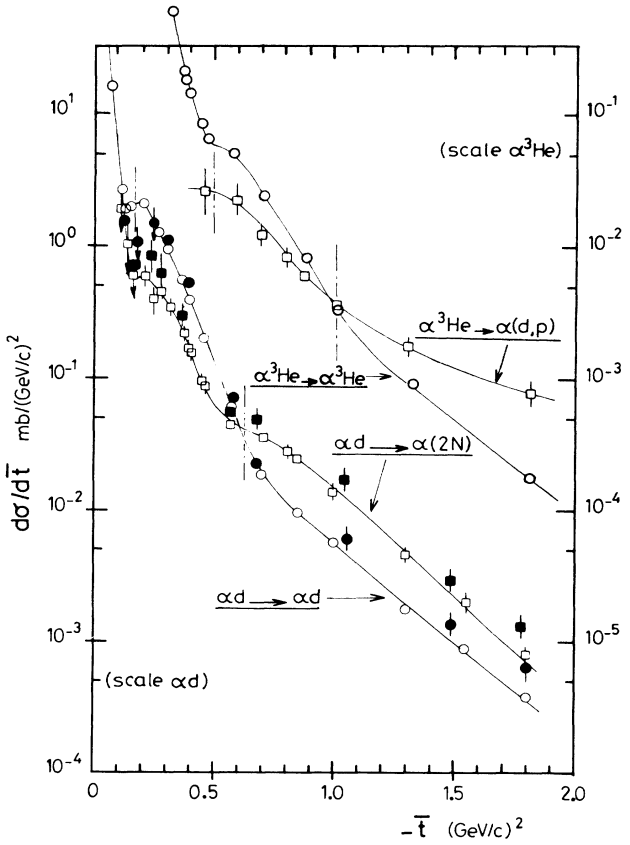

FIG. 8. $d\sigma/d\bar{t}$ integrated partial cross sections for αd$\rightarrow\alpha(2N)$ at 7 GeV/c (□) and 4 GeV/c (■), along with αd$\rightarrow\alpha$d at the same energies, 7 GeV/c (○) and 4 GeV/c (●); and for $\alpha\,^3$He$\rightarrow\alpha$(d,p) and $\alpha\,^3$He$\rightarrow\alpha\,^3$He at 7 GeV/c. The lines are to guide the eye.

ing. Indeed, the position of the diffractive structure at lower momentum transfer than the calculated value can be understood by the contribution of the quasielastic scattering of α's on multibaryonic substructures, which is not taken into account in the calculations, minima of diffraction of the corresponding partial spectra occurring at lower momentum transfers.

On the other hand, with regard to the cross sections at high momentum transfers, as will be noted in the discussion that follows, the Glauber models seem to underestimate low orders of scattering for αN quasielastic reactions, and the interference contributions taken into account are probably excessive.

Finally, the superposition of αp elastic cross sections on the αd inelastic spectrum shows the preponderance of αN reactions at low transfers and the importance of double scattering after the first minimum (Fig. 11).

IV. THEORETICAL COMMENTS AND INTERPRETATION OF THE INTEGRATED PARTIAL SPECTRA

A. αN+spectator quasielastic scattering

In Fig. 5 we observed the superposition of the αN quasielastic cross sections on the αp elastic cross sections measured in the same experiment. This effect is predicted by multiple scattering models at low transfers, but it is unexpected beyond the first minimum. Thus, calculations by Fujita and Hüfner using the multiple scattering series of Glauber and Matthiae[13] predict that multiple scattering must dominate at high transfers. In the same way, combining Glauber formalism with the Thomas-Reiche-Kuhn sum rule to calculate mean energy loss in the reaction $\alpha\alpha \rightarrow \alpha X$, Krimm *et al.*,[3] as well as Simbel *et al.*,[5] predict that multiple scattering on several nucleons must play a leading role at high momentum transfers. Our data at 7 GeV/c lead us to a different conclusion. This is also obvious from Fig. 12, where these calculations[3,5] are compared with the mean energy loss of the spectra measured. As can be seen from this figure, it is only when α scattering on one nucleon passes by a minimum ($q^2/2m_p \simeq 0.1$ GeV) that the weight of the scattering on several nucleons may dominate.

On the other hand, the fact that the αN quasielastic cross sections are always close to the αp elastic cross sections, up to the higher momentum transfers, is possi-

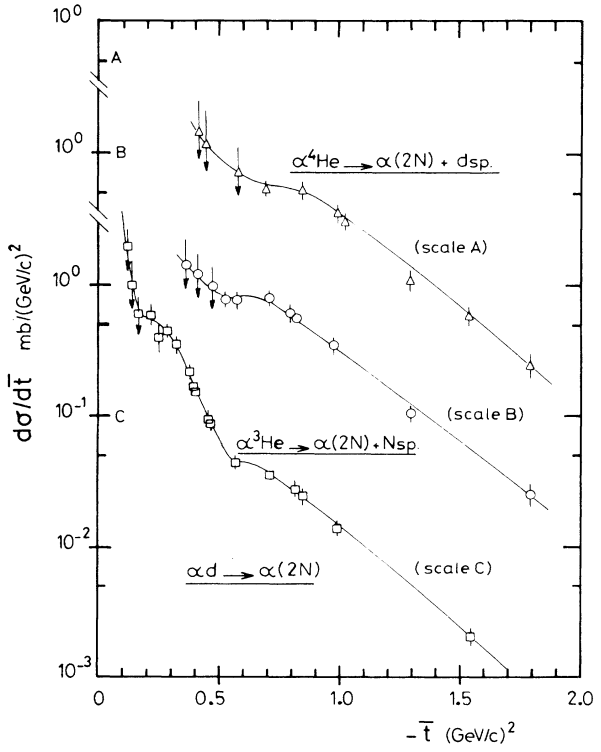

FIG. 9. $d\sigma/d\bar{t}$ integrated partial cross sections at 7 GeV/c for $\alpha\,^4\text{He} \rightarrow \alpha(2\text{N}) + \text{d}$ spectator and for $\alpha\,^3\text{He} \rightarrow \alpha(2\text{N}) + \text{N}$ spectator, along with $\alpha\,^2\text{H} \rightarrow \alpha(2\text{N})$. Data are spaced out to enhance legibility. The solid lines are to guide the eye.

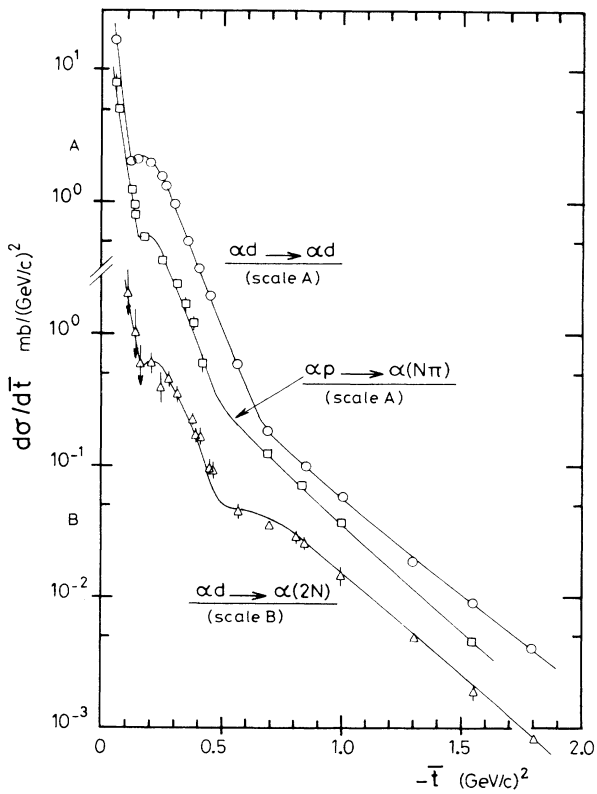

FIG. 10. $d\sigma/d\bar{t}$ cross sections for the reaction $\alpha\text{p} \rightarrow \alpha(\text{p},\pi)$ corresponding to the evaluation proposed in the text [integration of spectra A, as represented in Fig. 4(a)]. Here these cross sections are compared with αd elastic cross sections and with $\alpha\text{d} \rightarrow \alpha(2\text{N})$ cross sections; the $\alpha(2\text{N})$ spectrum is spaced out by a factor of 10 to enhance legibility. The solid lines are to guide the eye.

ble only if the interference contributions are negligible. Therefore, not taking into account this effect in the analysis of these data is justified.

B. Quasielastic scattering of αd and αt with a spectator

As was shown with our first $\alpha\alpha$ data,[1] the integrated cross sections $d\sigma/d\bar{t}$ for the following quasielastic reactions,

$\alpha\alpha \rightarrow$ d + d spectator ,

$\alpha\alpha \rightarrow$ t + N spectator ,

$\alpha\,{}^3\mathrm{He} \rightarrow \alpha$ + N spectator ,

can be described at low transfer by the Czyz and Maximon model.[9] At high transfer momentum, the predictive capacities of this model are only qualitative, even for elastic scattering.[8] But, when the calculations are adjusted to the data in the range of transfer where this model fits the elastic reactions well, we can determine two characteristics of the substructures concerned:

(i) The mean square radius of the substructure. This result occurs through the wave functions used in the calculations. These functions are harmonic oscillator wave functions, which appear in the form of a nuclear density dependent on a parameter R, i.e.,

$$\rho(r)=(\pi/R^2)^{3/2}\exp(-r^2/R^2) \quad \text{with } R^2=\tfrac{2}{3}\langle r^2\rangle \ .$$

(ii) The "spectroscopic factor" f of the scattered substructure, if we consider that this result can be obtained by determining the scale factor between the curve calculated and the experimental cross sections $d\sigma/d\bar{t}$.

The best fits of the cross sections $d\sigma/d\bar{t}$ for the reactions $\alpha\alpha \rightarrow$ d + d spectator and $\alpha\alpha \rightarrow$ t + N spectator at 7 GeV/c are obtained with the same values proposed to describe these spectra at lower energy,[1] that is,

(a) for a "dibaryon" in ^{4}He, $\langle r_d^2\rangle \simeq (1.0\ \mathrm{fm})^2$ and $f_d \sim 0.5$, and

(b) for a "tribaryon" in ^{4}He, $\langle r_t^2\rangle \simeq (1.2\ \mathrm{fm})^2$ and $f_t \simeq 0.5$.

Cross sections for $\alpha\,{}^3\mathrm{He} \rightarrow \alpha$ + N spectator are also reproduced at lower transfer with the same Glauber calculation, but this time with $\langle r_d^2\rangle \simeq (1.4\ \mathrm{fm})^2$ and $f_d \simeq 1$. This "spectroscopic factor" seems to mean that the "dibaryon" in ^{3}He behaves as a quasifree deuteron.

The results of these fits are presented in Figs. 6 and 7. The fits of the elastic cross sections using this model, shown in the same figures, indicate that this calculation is valid in the same low momentum transfer range for both elastic and quasielastic cross sections.

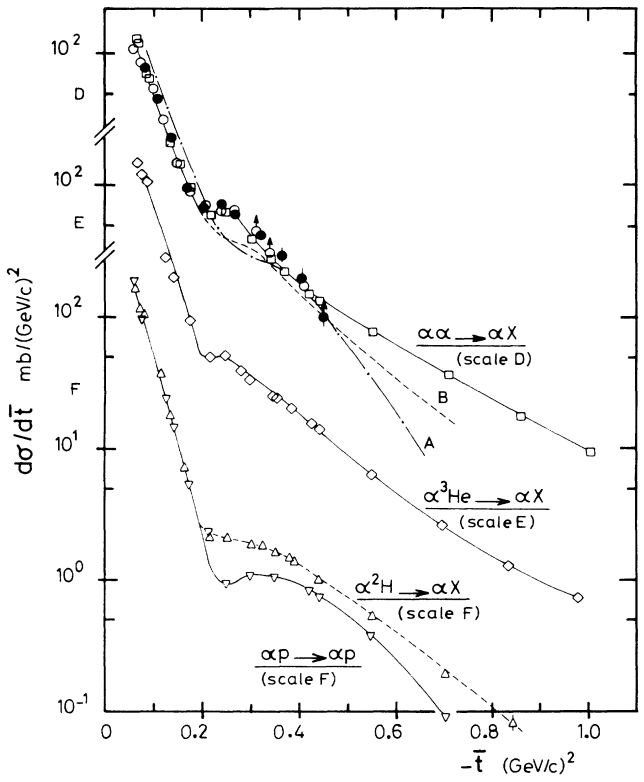

FIG. 11. $d\sigma/d\bar{t}$ integrated inclusive inelastic cross sections for $\alpha\alpha \rightarrow \alpha$X at 4.32 GeV/$c$ (○), 5.07 GeV/c (●), and 7 GeV/c (□). The dashed lines A and B on the $\alpha\alpha$ spectra are theoretical calculations from Refs. 3 and 4. Also shown are $d\sigma/d\bar{t}$ integrated inelastic cross sections for $\alpha\,{}^3\mathrm{He} \rightarrow \alpha$X at 7 GeV/$c$ (◇) and $d\sigma/d\bar{t}$ integrated cross sections for $\alpha\,{}^2\mathrm{H} \rightarrow \alpha$X at 7 GeV/$c$ (△), along with αp elastic cross sections at the same energy (▽). Lines between data dots are to guide the eye.

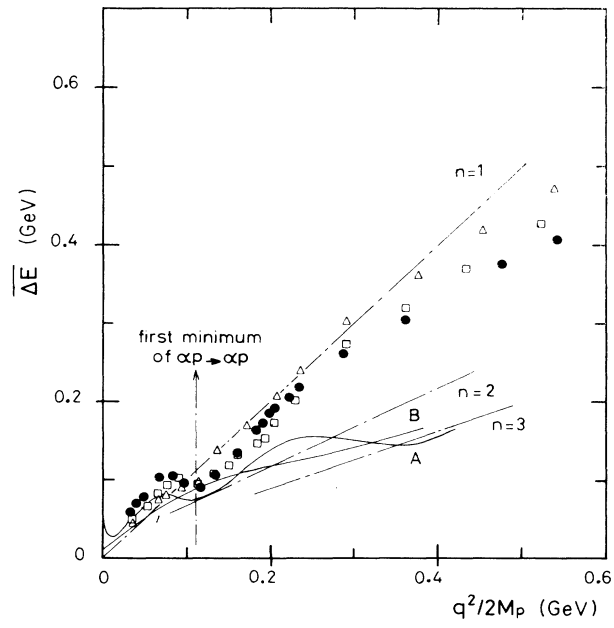

FIG. 12. Mean energy loss $\overline{\Delta E}$ vs $\rho=(q^2/2M_p)$ for α nucleus $\rightarrow \alpha$X at 7 GeV/c. The solid lines A and B are the results of calculations from Refs. 3 and 5. The dashed lines represent the mean energy loss for $n=1$, 2, and 3 collisions in the target, according to the calculation from Ref. 3. ●, for $\overline{\Delta E}$ in $\alpha\alpha \rightarrow \alpha$X; □, for $\overline{\Delta E}$ αt $\rightarrow \alpha$X; △, for $\overline{\Delta E}$ αd $\rightarrow \alpha$X.

The dominance of quasielastic processes with twofold breakup of the target, one of the two components being a spectator, is also shown by Rock *et al.*[14] They use the "quark-spectator counting rules" generalization for nucleons in the nuclei[15] to account for inelastic electron scattering on ^{3}He and ^{4}He.

C. Double scattering processes

The importance of this new contribution has already been shown in our first measurement of the reaction $\alpha d \rightarrow \alpha X$ at 4 GeV/c incident momentum.[12,16] We also observe this effect in the reaction $dd \rightarrow dX$ at 3 GeV/c. Ballot *et al.*[17,18] tried to calculate this process in the framework of the multiple scattering formalism; the calculations give too many structures produced by complicated interferences, while the experimental cross sections are smooth and globally higher than calculated values.

CONCLUSIONS

It has been shown that the different scattering processes occurring in α inclusive inelastic scattering data at 7 GeV/c can be identified. Besides weak pion production, these various processes correspond only to simple elastic scatterings on substructures of the targets and quasielastic scatterings on two substructures; neither multiple scattering of a higher order nor interference effects are needed to describe these data.

The elastic behavior of the partial reaction is stressed by the most striking feature of the corresponding cross sections, i.e., the clear diffraction structures of these spectra. This behavior is corroborated by the similarities between these spectra and those of the elastic reactions measured in the same experiments and also by the fact that quasielastic cross sections can be fitted at low transfer momentum by a similar theoretical model assigned to the elastic reactions. This Czyz and Maximon model enables us both to confirm the mean square radii and the spectroscopic factors of the substructures of ^{4}He, previously deduced from $\alpha\alpha$ data at lower energy, and now also to determine the corresponding values for the substructures of ^{3}He.

We find it remarkable that the resulting cross sections for the quasielastic reaction αN (+ spectator) are close to those for the αp elastic reaction. This process, which is true for all the light targets studied and up to the highest momentum transfers measured, was not foreseen by the multiple scattering theories.

The fact that there is no significant interference effect contribution can be simply explained; in the final state of each partial reaction, either the substructures are different, or the kinematic properties are different, or both, and only the cross sections add up, but not the amplitudes.

Pion production can also be understood as a quasielastic process analogous to the double quasielastic reaction $\alpha d \rightarrow \alpha(2N)$, with a pion taking the place of a nucleon. By comparing single pion production measured in the same experimental conditions with a ^{2}H, ^{3}He, and ^{4}He target, it is possible to evaluate the inelastic contributions, in spite of the low cross sections for these reactions.

Now, a better understanding of such data, particularly at high momentum transfer, will require a good theoretical model for elastic scattering phenomena. The substructures in the nuclei will probably have to be taken into account in this theory.

An extension of this study to heavier nuclei would be very interesting, but unfortunately we have seen that analysis of the inclusive spectra rapidly becomes difficult and lacks precision when the atomic number of the target is increased. The study of such processes would be possible if at least some of the scattered elements were also detected. In spite of new experimental difficulties, the increase in our knowledge of nuclei heavier than ^{4}He would justify such an undertaking.

The author wishes to thank Dr. V Franco, Dr. J. Hüfner, and Dr. A. Tekou for stimulating and very helpful discussions.

[1] J. Duflo *et al.*, Nucl. Phys. **A356**, 427 (1981).
[2] T. Fujita and J. Hüfner, Phys. Lett. **87B**, 327 (1979).
[3] H. Krim *et al.*, Nucl. Phys. **A367**, 333 (1981).
[4] A. Malecki *et al.*, Phys. Lett. **136B**, 319 (1984).
[5] H. Simbel *et al.*, Phys. Lett. **94B**, 11 (1980).
[6] J. Banaigs *et al.*, Phys. Rev. C **35**, 1416 (1987).
[7] J. Banaigs *et al.*, Nucl. Phys. **A445**, 737 (1985).
[8] L. Satta *et al.*, Phys. Lett. **139B**, 263 (1984).
[9] W. Czyz and L. C. Maximon, Ann. Phys. (N.Y.) **52**, 117 (1969).
[10] J. Berger *et al.*, Nucl. Phys. **A260**, 421 (1980).
[11] F. Krebs *et al.*, Nucl. Phys. **A395**, 384 (1983).
[12] A. I. Yavin, Nucl. Phys. **A374**, 297 (1982).
[13] R. Glauber and G. Matthiae, Nucl. Phys. **B21**, 135 (1970); W. Czyz and L. C. Maximon, Ann. Phys. (N.Y.) **52**, 117 (1969).
[14] S. Rock *et al.*, Phys. Rev. C **26**, 1592 (1982).
[15] J. Brodsky and B. T. Chertok, Phys. Rev. D **14**, 3003 (1976).
[16] B. Marini, thèse troisème cycle, Université de Caen, 1979.
[17] M. P. Combes *et al.*, Nucl. Phys. **A431**, 703 (1984).
[18] J. L. Ballot *et al.*, Nucl. Phys. **A431**, 710 (1984).